



Minerva Access is the Institutional Repository of The University of Melbourne

Author/s:

Sullivan, SA;Orosco, JC;Callejas-Hernández, F;Blow, F;Lee, H;Ranallo-Benavidez, TR;Peters, A;Raidal, SR;Girard, YA;Johnson, CK;Rogers, KH;Gerhold, R;Mangelson, H;Liachko, I;Srivastava, H;Chandler, C;Berenberg, D;Bonneau, RA;Huang, PJ;Yeh, YM;Lee, CC;Liu, H;Chen, TW;Tang, P;Chiu, CH;Schatz, MC;Carlton, JM

Title:

Comparative genomics of the parasite *Trichomonas vaginalis* reveals genes involved in spillover from birds to humans

Date:

2025-12-01

Citation:

Sullivan, S. A., Orosco, J. C., Callejas-Hernández, F., Blow, F., Lee, H., Ranallo-Benavidez, T. R., Peters, A., Raidal, S. R., Girard, Y. A., Johnson, C. K., Rogers, K. H., Gerhold, R., Mangelson, H., Liachko, I., Srivastava, H., Chandler, C., Berenberg, D., Bonneau, R. A., Huang, P. J., ... Carlton, J. M. (2025). Comparative genomics of the parasite *Trichomonas vaginalis* reveals genes involved in spillover from birds to humans. *Nature Communications*, 16 (1), pp.6487-. <https://doi.org/10.1038/s41467-025-61483-w>.

Persistent Link:

<https://hdl.handle.net/11343/363369>

License:

[CC BY-NC-ND](#)


Comparative genomics of the parasite *Trichomonas vaginalis* reveals genes involved in spillover from birds to humans

Received: 5 January 2025

Accepted: 23 June 2025

Published online: 24 July 2025


 Check for updates

Steven A. Sullivan^{1,2,22}, Jordan C. Orosco^{1,2,22}, Francisco Callejas-Hernández^{1,2}, Frances Blow ^{1,15}, Hayan Lee ^{3,16}, T. Rhyker Ranallo-Benavidez ^{4,17}, Andrew Peters⁵, Shane R. Raidal⁶, Yvette A. Girard^{7,18}, Christine K. Johnson ⁷, Krysta H. Rogers⁸, Richard Gerhold⁹, Hayley Mangelson¹⁰, Ivan Liachko¹⁰, Harsh Srivastava^{1,2}, Chris Chandler¹, Daniel Berenberg¹¹, Richard A. Bonneau ^{1,19}, Po-Jung Huang¹², Yuan-Ming Yeh ^{12,20}, Chi-Ching Lee¹², Hsuan Liu¹², Ting-Wen Chen ^{12,21}, Petrus Tang^{12,13}, Cheng-Hsun Chiu¹³, Michael C. Schatz⁴ & Jane M. Carlton ^{1,2,14} 

Trichomonas vaginalis, the causative agent of the venereal disease trichomoniasis, infects men and women globally and is associated with serious outcomes during pregnancy, increased risk of HIV-1 infection, and cancers of the human reproductive tract. Species of trichomonad parasitize a range of hosts in addition to humans, including birds, livestock, and pets. Genetic analysis of trichomonads recovered from columbid birds has provided evidence that they undergo frequent host-switching, and that a spillover event from columbids likely gave rise to *T. vaginalis* in humans. Here we describe a comparative genomics study of seven trichomonad species, generating chromosome-scale reference genomes for *T. vaginalis* and its avian sister species *Trichomonas stableri*, and assemblies of five other species that infect birds and mammals. Human-infecting trichomonad lineages have undergone recent and convergent genome size expansions compared to their avian sister species, a result of extensive repeat expansions specifically of multicopy gene families and transposable elements, with genetic drift likely a driver due to relaxed selection. Trichomonads are thought to have independently host-switched twice from birds to mammals/humans. We identify gene functions implicated in the transition, including host tissue adherence and phagocytosis, extracellular vesicle formation, and CAZyme virulence factors, which are all associated with pathogenesis phenotypes.

Trichomoniasis, the most prevalent non-viral venereal disease of humans¹, is caused by the protozoan *Trichomonas vaginalis* that infects the lower genital tract of men (urethra and prostate) and women (vulva, vagina, and cervix). Symptoms include foul-smelling vaginal discharge and genital itching, and infections are associated

with an increased risk of cervical and prostate cancer, HIV-1 infection, and complications during pregnancy². Other human-infecting trichomonads include the oral parasite *Trichomonas tenax* associated with periodontal disease³, and the intestinal parasite *Pentatrichomonas hominis* associated with gastrointestinal distress and diarrhea⁴.

A full list of affiliations appears at the end of the paper.  e-mail: JaneCarlton@jhu.edu

Trichomonad species also infect a wide range of vertebrate hosts, including birds, livestock, and pets. *Trichomonas gallinae*⁵ infects the upper gastrointestinal (GI) tract of birds, including doves, pigeons, songbirds, and raptors that prey on infected birds, and is responsible for a large decline of greenfinch and chaffinch populations in Great Britain in the early 2000s⁶. In 2008, novel parasites with highly genetically similar markers to *T. vaginalis* (dubbed “*T. vaginalis*-like”) were reported in white-winged doves and mourning doves from Arizona and Texas, and in Pacific coast band-tailed pigeons from California⁷. *T. vaginalis*-like parasites recovered from the latter during a 2011–12 outbreak were analyzed in detail and given the species name *Trichomonas stableri*⁸. *T. vaginalis* may have originated as a zoonosis from American pigeons and doves during a spillover event following human colonization of the Americas⁹. It has been hypothesized that its ancestor moved from the upper GI tract of columbids into the human reproductive tract via barrier contraceptives or more commonly through human contact with bird-infected water⁹.

A draft *T. vaginalis* whole genome sequence generated using Sanger sequencing in 2007¹⁰ revealed a highly repetitive genome comprised of thousands of highly similar transposable elements (TEs) and many multicopy gene families. The ~180 Mb genome size was unexpectedly large compared to other human mucosal parasite genomes e.g., *Giardia* (~11 Mb) and *Entamoeba* (~21 Mb)¹¹. Extreme fragmentation of the assembly (> 64,000 scaffolds and contigs) precluded accurate counting of repetitive elements. However the sequence generated insights into (1) multicopy gene families involved in the parasite’s active endocytic and phagocytic life-style such as protein kinases and peptidases; (2) surface proteins including the highly diverse BspA-like proteins that likely mediate parasite adherence to vaginal epithelial cells required to establish and maintain an infection in the reproductive tract; and (3) novel metabolic pathways shaped by putative prokaryote-to-eukaryote lateral gene transfer (LGT) events. Other trichomonad genomes remained largely unsequenced, although in the interim, molecular phylogenies showed avian trichomonads to be the closest known relatives of *T. vaginalis* and *T. tenax*^{7,12}, with columbids inferred to be the ancestral host of the genus, and the source of at least two independent host switches to mammals/humans⁹. Host switching has been posited to be a strong macro-evolutionary force in genus *Trichomonas*⁹.

To expand the number of available trichomonad genome sequences, address key knowledge gaps in the evolution of the parasite, and identify genes implicated in the spillover event from avian to human host, we leveraged long-read and chromosomal conformation sequencing to generate chromosome-scale reference genome assemblies for *T. vaginalis* G3 and its sister species the avian parasite *T. stableri*. We used short-read sequencing to also assemble draft genomes of two other human-infecting species, *T. tenax* and *P. hominis*, and three other bird-infecting species. These seven assembled genomes represent an extensive whole genome sequence dataset of trichomonads, and enabled unique comparative genomics, including estimates of gene and TE content in closely-related species from different hosts, and visualization of synteny. We offer insights into trichomonad evolution, including evidence for relaxed selection accompanying the inferred host switch from birds in two human-infective *Trichomonas* lineages, which likely explains the striking genome size variation among these trichomonads. Finally, we identify convergently evolving genes in human-infecting species that were putatively involved in the transition from bird to human host.

Results

Comprehensive TE annotation of a new *T. vaginalis* chromosome-scale assembly

We generated a chromosome-scale reference assembly of *T. vaginalis* strain G3 using Pacific Bioscience long-read sequencing augmented with chromosome conformation capture (‘PacBio/Hi-C’). The assembly

comprises six chromosome-scale scaffolds matching the published *T. vaginalis* karyotype number¹³ ranging from 20 to 40 Mb and ~177 Mb total length (in contrast to the 2007¹⁰ Sanger assembly of >64,000 scaffolds [range 0.2–585 kb] and 176 Mb total length). Microsatellite and rRNA loci localized to metaphase chromosome squashes by FISH^{10,14} were mapped to the assembly to assign chromosome numbers I–VI to the scaffolds (Fig. 1). We improved the accuracy of the *T. vaginalis* predicted proteome, identifying 37,794 protein-coding genes (Table 1), with 46% annotated as ‘hypothetical’ (compared to the 59,681 genes with 75% hypotheticals predicted in 2007¹⁰). Improved annotation of the 16 major multicopy gene families, many of which are associated with cell surface activity, parasite-host interactions, and the degradome, increased their copy numbers, more than quadrupling it in the case of cysteine peptidase Clan CA, family C1 (Supplementary Table 1). The >600 rDNA genes identified in 2007 collapsed to eleven 28S/5.8S/18S rRNA cassettes tandemly arrayed on chromosome II, agreeing with FISH results¹⁰ (Fig. 1). We extended a previously reported¹⁵ block of genes laterally transferred from a relative of the firmicute bacterium *Peptoniphilus harei*, from 37 Kb containing 27 genes to 47 Kb containing 45 genes (Supplementary Table 2). The *T. vaginalis* genome remains densely packed with protein-coding genes and TEs, with an average length of 1131 bp (median length 520 bp) between them.

TE sequences, difficult to identify and incompletely classified in the previous draft assembly, were meticulously annotated and found to dominate the new *T. vaginalis* reference genome, making up at least 46% of its length (Table 1 and Supplementary Fig. 1). While MULE TEs dominate by abundance (7322), more than 4700 Maverick (TvMav) TEs, long (~10–28 Kb) virus-like DNA transposons found in all major eukaryotic lineages except plants and mammals¹⁶, comprise >80% of the total TE length and ~40% of genome length (Table 2). We undertook extensive manual curation of TvMavs since they can contain as many as 19 TE genes, lack terminal inverted repeats (TIR), are concatenated or nested within each other, and can envelop other types of TEs¹⁶. Based on length, TIR sequence, gene repertoire, and gene order of 2788 well-defined TvMavs, we identified three classes. Class 1 ($n = 902$) and Class 2 ($n = 181$) range from 20 to 25 Kb and differ mainly in TIR sequence. The abundant and previously undescribed Class 3 ($n = 1705$) has a bimodal length distribution, suggesting two subclasses with peaks at 10–20 Kb and 23–26 Kb (Supplementary Fig. 2). Class 3 also has a distinct gene repertoire and order (Supplementary Tables 3–5).

Comparative genomics of trichomonads infecting humans, birds, and mammals

We chose several species within genus *Trichomonas* known to be closely related to *T. vaginalis* on the basis of single-copy gene phylogenies¹² for comparative evolutionary studies, including a more distantly related trichomonad species as an evolutionary outgroup. Growing parasites in vitro proved challenging and several could not be grown continuously or in sufficient volume to generate the required quantity or quality of DNA for long-read sequencing. The final list of assembled species and their sequencing statistics is shown in Table 1: (1) the New World clade bird parasite *T. stableri* strain BTPI-3, the closest known relative of *T. vaginalis* sequenced using PacBio/HiC; (2) an Australasian bird parasite *Trichomonas* species genotype 1c (*T. sp.* 1c)⁹; (3) the Old World human parasite *T. tenax* Hs-4:NIH, (4) an Old World bird parasite *Trichomonas* species genotype 2a (*T. sp.* 2a), the closest known relative of *T. tenax*⁹, (5) the Old World bird parasite *Trichomonas gallinae* (TGAL)⁹; and (6) the human/mammal parasite *P. hominis* (Hs-3:NIH), used as an outgroup for our analyses. Genome size estimates calculated from short reads of the species ranged from 68.9 Mb for *T. gallinae* to 184.2 Mb for *T. vaginalis* (Table 1), the latter by far the largest genome size of the seven trichomonad species sequenced. The estimated genome size is larger for human-infecting

species than bird-infecting species. It exhibits a linear relationship to estimated repeat content (multicopy genes, TE sequences, and unclassified repeats), which ranges from 21.4% in *T. sp. 2a* to 68.6% in *T. vaginalis* (Supplementary Fig. 3). Estimated repeat contents of bird-infecting species (21%–37%) are far lower than those of human-infecting species (51%–69%). Counts of predicted protein-coding genes in the assemblies ranged from 23,689 (*T. sp. 1c*) to 37,794 (*T. vaginalis*) and did not display associations with genome size or host type (Table 1).

Pairwise whole genome DNA alignments of the species confirmed several previously proposed relationships^{7–9}, including the presence of two lineages that exhibit close ‘sister species’ relationships between a human-infecting species and a bird-infecting species (human *T.*

vaginalis with bird *T. stableri*; and human *T. tenax* with bird *T. sp. 2a*) (Supplementary Fig. 4). Whole chromosome synteny mapping of *T. vaginalis* with its avian sister species *T. stableri* showed large differences in chromosome sizes and massive genome rearrangements (Fig. 2).

We identified 24,465 orthogroups (groups of evolutionarily related genes) across the seven trichomonad species, with 93.8% of all genes being assigned to an orthogroup. Of these orthogroups, 10,457 contain genes from all species (Fig. 3A), 6226 contain only single-copy genes, and 2798 orthogroups, comprising 6.6% of all genes, are species-specific. As expected, the outgroup *P. hominis* contained the largest number of species-specific orthogroups (1078), followed by *T. vaginalis* (425). We used the 6226 single-copy orthologs to infer a



Fig. 1 | Architecture and genome features of *T. vaginalis* G3 across its six chromosomes. The concentric rings, from innermost to outermost, represent: (1) chromosome size in Mb; (2) gene density (green plot) shown in 20 Kb windows; vertical blue lines represent 11 rRNA cassettes, and the vertical black line represents the 47.5 Kb block from an LGT event of the bacterium *Peptoniphilus hareii*; (3) TE

density (pink plot) shown in 20 Kb windows; (4) transcript abundance (brown plot) of all genes shown as transcripts per million (TPM) in 100 Kb windows; (5) TE transcript abundance (orange plot) of annotated TE genes shown as TPM in 100 Kb windows; and (6) dN/dS values (grey dots). The axes are shown next to chromosome I.

Table 1 | Genome assembly and annotation statistics for seven trichomonad species

Strain name (ATCC identifier)	<i>Trichomonas vaginalis</i>	<i>Trichomonas stableri</i>	<i>Trichomonas tenax</i>	<i>Trichomonas sp. geno-type 1c</i>	<i>Trichomonas sp. geno-type 2a</i>	<i>Trichomonas gallinae</i> ^a	<i>Pentatrichomonas hominis</i>
	G3 (ATCC PRA-98)	BTPI-3 (ATCC PRA-412)	Hs-4:NIH (ATCC 30207)	TTHO	TTEN	TGAL	Hs-3:NIH (ATCC 30000)
Isolation details, year	Female urogenital tract, Kent, United Kingdom, 1973	Band-tailed pigeon (<i>Patagioenas fasciata</i>), California, 2008	Human adult female subgingival space, 1959	Wonga pigeon (<i>Leucosarcia picata</i>), Batemans Bay, NSW, Australia, 2011	Barred-shouldered dove (<i>Geopelia humeralis</i>), Fingal Head, NSW, Australia, 2011	Domestic rock dove (<i>Columba livia</i>), Carabost, NSW, Australia, 2011	Human intestine, Korea, 1950
Host range	Human	Bird	Human, cat, dog, (bird)	Bird	Bird	Bird	Human, cat, dog, monkey, guinea pig
Platform	PacBio + HiC	PacBio + HiC	Illumina	Illumina	Illumina	Illumina	Illumina
Estimated genome size (Mb)^b	184.2 ^c	73.0 ^d	104.9	77.8	81.0	68.9	100.2
Assembly size (Mb)^b	181.5 ^c	72.3 ^d	70.4	55.4	72.5	55.7	54.3
Assembly statistics	six scaffolds (176.6 Mb), 212 contigs (4.7 Mb)	six scaffolds	35,468 contigs	13,785 contigs	13,690 contigs	8,409 contigs	18,431 contigs
N50 (bp)	34.7 Mb (9.240 ^b)	14.5 Mb (11.033 ^b)	11,499	18,842	22,721	28,086	10,851
Repeat content (%)^b	68.6 ^e	32.6 ^d	50.6	36.6	21.4	25.8	53.7
% GC	32.7	31.2	34.1	29.8	34.4	33.7	37.8
No. predicted genes (excluding TEs)	37,794	28,579	29,838	23,689	33,504	24,752	26,270
No. predicted TEs	20,720 ^e	625 ^f	459 ^g	254 ^g	150 ^g	164 ^g	897 ^h

^aSee Supplementary Methods for further description.

^bEstimated from short-read Illumina sequence data using GenomeScope³¹.

^cCalculated from short-read Illumina sequence data of *T. vaginalis* strain CDC 085 to provide comparable statistics to other species sequenced using the same sequencing platform.

^dCalculated from short-read Illumina sequence data of *T. stableri* strain CA015840 to provide comparable statistics to other species sequenced using the same sequencing platform.

^eDerived from BLAST searches; a TE was counted if it contained at least one gene, which excluded numerous short TE-derived sequences.

^fDerived from BLAST searches and RepeatModeler.

^gEstimated using DeviateTE³².

^hATCC American Type Culture Collection.

Table 2 | Total number of elements in nine of the most common TE families found in seven trichomonad genomes

	Avg. length (bp)	<i>T. vaginalis</i>	<i>T. stableri</i>	<i>T. tenax</i> ^a	<i>P. hominis</i> ^b	<i>T. sp.2a</i>	<i>T. sp.1c</i>	<i>T. gallinae</i>
Harbinger	2800	48	14	3	48	10	2	7
hAT	2000	243	197	13	154	22	50	20
Helitron	5000	2	27	9	1	1	67	9
IS-like	1100	4038	371	9	8	15	17	13
Kolobok/Bac	1500	2536	16	15	7	3	6	14
Mariner	1300	891	176	15	247	47	61	32
Maverick	16,000	4714	86	254	363	7	7	54
MULE	2200	7322	57	13	38	14	33	6
NeSL	4400	5	7	127	31	31	11	10
Unclassified	ND	762	8	ND	ND	ND	ND	ND
Total		20,561	625	459	897	150	254	164

Average lengths are derived from those exhibited by *T. vaginalis* TEs. *T. vaginalis* and *T. stableri* genomes were generated by long-read sequencing; all others are short-read assemblies. Icons show host species and bracket endpoints indicate inferred sister species on the phylogenetic tree in Supplementary Fig. 5.

ND not determined.

^a*T. tenax* has been detected in other mammals and in birds.

^b*P. hominis* has been detected in other mammals.

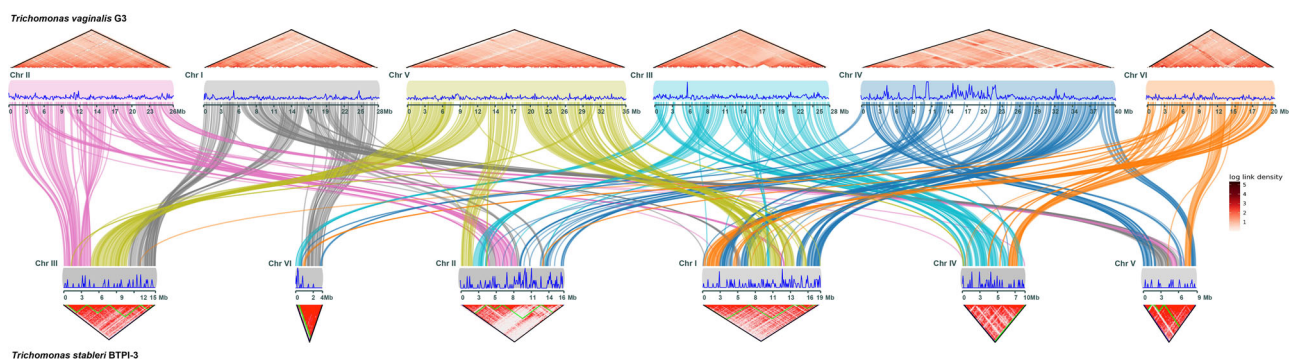


Fig. 2 | Synteny plot of human parasite *T. vaginalis* and its closest relative in birds *T. stableri*. Each of the six *T. vaginalis* chromosomes I–VI are colored uniquely, and synteny blocks between the two species are indicated by ribbons connecting the chromosomes. Chromosomes are not shown in numbered order for visualization purposes. Blue graph plots show normalized TE density (genomic

sequence classified as containing TEs) in 100 Kb windows on the top and bottom of each species' chromosomes. Hi-C interaction maps are shown as red triangles above (*T. vaginalis*) and below (*T. stableri*) the TE density plots, with lengths of contigs from the assemblies shown as white squares for *T. vaginalis* and green squares for *T. stableri*.

phylogenetic species tree (Supplementary Fig. 5). The tree strongly supports separate clades for *T. vaginalis* and *T. tenax*, in accordance with the proposal of at least two bird-to-human host switches in the evolutionary history of genus *Trichomonas*⁹. It also resolves the formerly ambiguous placement, from single-gene trees, of Australasian bird parasite *T. sp. 1c* among the Old or New World clades⁹; we find strong support for placing *T. sp. 1c* with the New World clade.

The burden of repeats/TEs in trichomonads differs by host type

The correlations between genome size, host type, and repeat content noted above are not necessarily reflected in phylogenetic proximity; for example, the human-infecting trichomonad lineages (*T. vaginalis*, *T. tenax*, *P. hominis*), while not closely related by evolution, all appear to have undergone recent and convergent large genome size expansions compared to their avian sister species (Fig. 3B). Kmer-based estimates of genome size and repeat content from sequencing reads clearly mark the three human-infecting species as having larger and more repetitive genomes than the bird-infecting species (Table 1). This is borne out in a comparison of the two long-read

assemblies, whose lengths concur with kmer-based estimates, and whose counts of repeat sequences are the most reliable: the major contributor to the much larger genome size of *T. vaginalis* versus *T. stableri* is increased repeat content, particularly expansion of TEs (Supplementary Fig. 1).

We identified and classified 22,449 TEs in *T. vaginalis*, 3443 in *T. stableri*, and, within the limits imposed by short-read assembly, 897 in *P. hominis*, 459 in *T. tenax*, and <300 in each of the bird-infecting species (Tables 1 and 2), again showing a human/bird host disparity. The great majority of TEs identified in all species are Class II DNA transposons, with a single Class I NeSL retrotransposon family identified as particularly abundant in *T. tenax* (Fig. 3B). Mavericks appear to be more abundant in the three human-infecting species *T. vaginalis*, *T. tenax*, and *P. hominis* than the bird species, since their size often makes them the dominant TE class by length, even when it is not the most abundant class (Supplementary Fig. 6), but no pattern of abundance was seen in other TE classes.

A closer inspection of the synteny between *T. vaginalis* with its sister species *T. stableri* in birds (Fig. 2) revealed the syntenic regions in

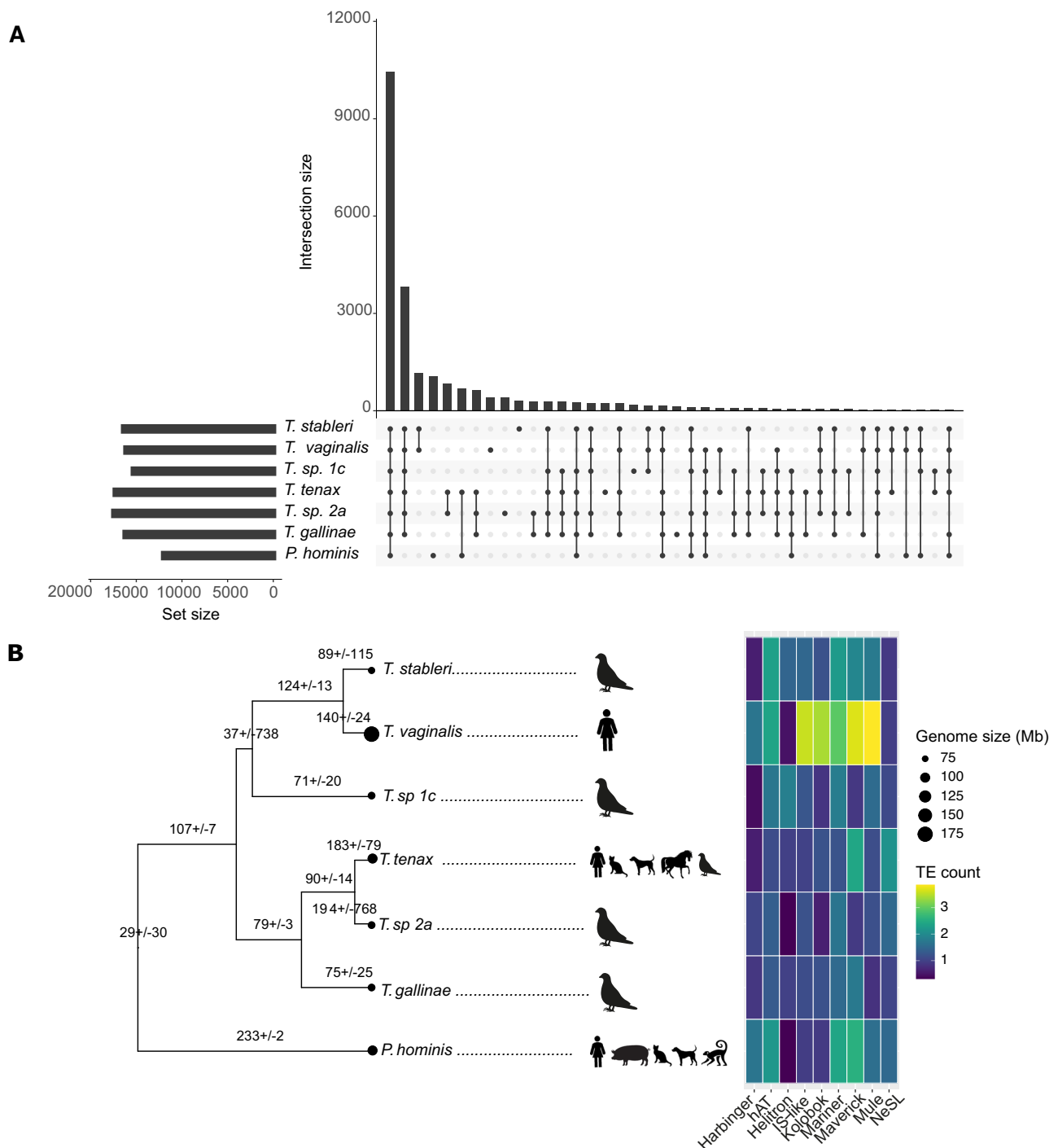


Fig. 3 | Genome content distribution. A An Upset plot displaying the intersection of orthogroups identified in OrthoFinder across seven trichomonad species. Each vertical bar represents the number of orthogroups shared at each species intersection, the set size indicates the number of orthogroups found in each species, and the connected dots represent the species in the intersection. **B** Ultrametric tree

from 6226 concatenated single-copy genes. Black dots at terminal nodes are proportional to estimated genome size, and hosts are denoted by cartoons. Estimated gene family expansions/contractions from 12,345 genes are denoted as + or – values on the tree. The heatmap shows the log₁₀ transformed count of TE family members for each tree branch.

T. vaginalis to be made up of almost equal numbers of TEs (47.3%) and non-TE (52.7%) protein-coding genes, whereas in *T. stableri* the regions are made up of 90.22% non-TE protein-coding genes (Supplementary Table 6). Analysis of the *T. vaginalis* protein-coding genes that are not TEs in the syntenic regions revealed many of them to be members of multicopy gene families enriched in gene ontology (GO) functions such as protein kinases, ATP/GTP binding, and protein phosphorylation. Copy numbers of several gene families are

markedly higher in *T. vaginalis* than *T. stableri*, e.g., the BspA-like (73% higher), Saposin-like (SAPLIP) (65% higher), and leishmanolysin-like proteinase (64% higher) families (Supplementary Table 7), signifying that these expansions were favored in the human host. Most of the remaining gene families, e.g., membrane trafficking proteins, serine peptidases, protein kinases, vary <10% in copy number between the two species, suggesting their gene duplications largely predate the bird-human host switch.

Relaxed selection supports a neutral model for genome expansion in human-infecting trichomonads

To assess levels of genetic drift (a nonadaptive possible driver of expansion of repetitive DNA when selection is relaxed) we used the hypothesis-testing framework RELAX¹⁷, which asks whether the strength of natural selection has been relaxed or ‘intensified’ (i.e., inferred to have undergone either purifying or positive selection) along specified test branches compared to reference branches in a phylogenetic tree. We used the 6226 single-copy orthologs occurring in all seven species as a proxy for genome-wide sampling of drift. With human-infecting branches as test (foreground) and avian branches as reference (background), we determined which genes evinced significant ($p < 0.05$) relaxed or intensified selection and found that human-infective branches have more genes under relaxed than intensified selection ($n = 894$ vs. $n = 494$) (Fig. 4A and Supplementary Data File 1), the converse of the bird-infecting branches.

A gene under relaxed selection may result from an organism switching environments if the gene is obsolete in the new host or tissue, or from increased genome-wide genetic drift (due to changes in parameters such as population size and mode of reproduction)¹⁸. To rule out host environment as the driver of observed relaxed selection, we used RELAX to test the strength of selection acting on 506 genes from the seven genomes with homology to BUSCO¹⁹ genes, since the rates of evolution of conserved genes are expected to remain constant even in different environments. We found that there are more genes under relaxed selection ($n = 47$) than intensified selection ($n = 44$) in the human-infecting species relative to bird-infecting species (Fig. 4A). This suggests a role for increased genome-wide genetic drift, rather than relaxed selection targeting genes that are superfluous in the new environment. Consistent with relaxed positive selection, the distribution of average dN/dS ratios (a measure of the strength and mode of natural selection acting on protein-coding genes) for the single-copy orthologs shows a higher median in avian-infecting parasites (7.318) and lower median in human-infecting parasites (5.786). We observed a higher median in avian-infecting parasites (0.585) and lower median in human-infecting parasites (0.542) for relaxed purifying selection (Fig. 4B). In general, therefore, dN/dS in human-infecting trichomonad species has contracted towards 1, i.e., neutral evolution.

T. vaginalis has the largest net gain of expanded multicopy gene families

We previously proposed that copy number expansions in *T. vaginalis* multigene families may account for a significant proportion of its unexpectedly large genome size compared to other parasites¹⁰. We investigated this further by analyzing *T. vaginalis* gene families in the context of our other assembled trichomonad genomes. We used CAFES²⁰, which implements a birth-death model for evolutionary inferences about gene family evolution, to identify multicopy gene families that have expanded or contracted significantly across our trichomonad phylogeny. Of the 26,244 orthogroups, 12,345 (see ‘‘Methods’’) were analyzed for expansions or contractions, of which 3853 showed significant expansions or contractions in at least one extant species or inferred ancestor (Fig. 3B and Supplementary Data File 1). We found that among the trichomonad species examined, *T. vaginalis* had the largest net gain ($n = 116$) in number of expanded gene families, consistent with it having undergone the largest genome size increase. The 140 expanded *T. vaginalis* gene families are functionally enriched in GO terms for transmembrane transport (e.g., ABC transporters), metabolism and translation (Fig. 5). We also identified many expanded gene families ($n = 61$) in *T. vaginalis* that have published functions related to parasite pathology, such as host cell adherence^{21–24}, phagocytosis²⁵, and extracellular vesicles^{26,27}. We did not find functional enrichment in the 24 multicopy gene families in *T. vaginalis* that have significantly contracted.

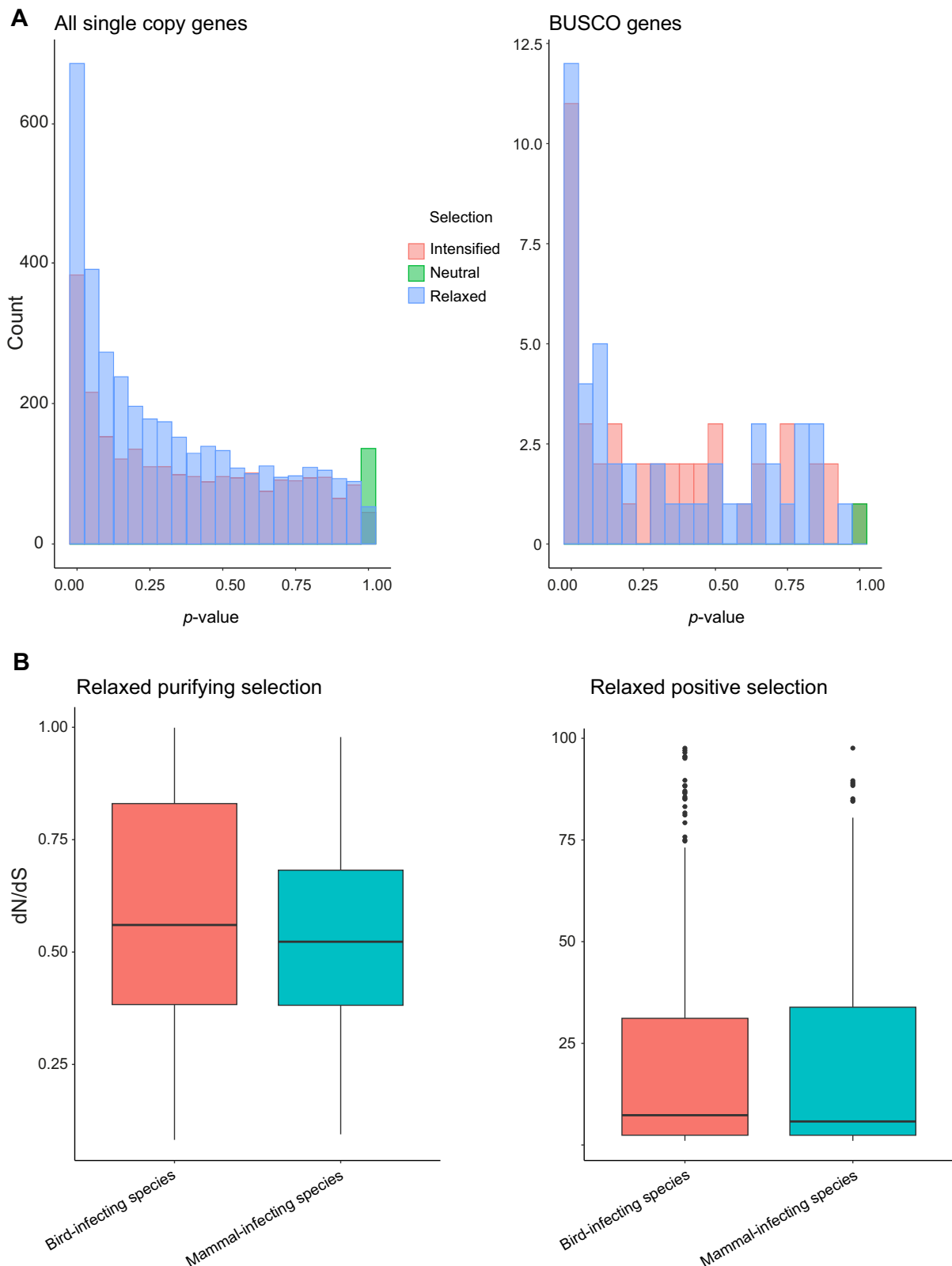
We found that *T. vaginalis* shares the largest number of expanded gene families not with its bird-infecting sister species *T. stableri*, but with human/mammal-infecting *T. tenax* ($n = 33$) and its sister species, bird-infecting *T. sp. 2a* ($n = 35$) (Fig. 6). These convergently expanded multicopy gene families of *T. tenax* and *T. vaginalis* are enriched for GO terms in metabolism, and include 25 genes previously reported to be associated with cell adherence^{21,22,28}, microvesicles^{26,29}, and putative virulence factors³⁰. *T. vaginalis* shares the largest number of expanded gene families with *T. sp. 2a* and consists of GO terms enriched in many biological processes such as transport, telomere maintenance, signal transduction, morphogenesis, and immune response. We similarly found genes with published associations with adherence and microvesicles, but to a lesser degree ($n = 13$). We also identified 15 convergently contracted multicopy gene families in *T. tenax* and *T. vaginalis* species (Supplementary Fig. 7), but without any GO term enrichment.

Trichomonas genes under positive selection and involved in bird-to-mammal/human host switch

We used a branch-site model implemented in aBRASEL³¹ to test the 6226 single-copy orthologs across our trichomonad species for evidence of positive selection (Supplementary Fig. 8 and Supplementary Data File 1). Approximately 18% of the 1201 genes with evidence of positive selection were shared between two or more species, the rest being specific to a single species. The shared genes were enriched in GO terms for translation, intracellular transport, and cytoskeleton/motility, most likely reflecting functions essential to trichomonads generally (Supplementary Fig. 9). A relatively large number of these shared genes have been previously associated with phagocytosis²⁵ ($n = 44$) and include proteases, cytoskeleton genes, transmembrane and transporter genes, vesicular trafficking, and metabolism-related genes, and a similar number were associated with microvesicles²⁶ ($n = 40$), including a number of tRNA synthetases and peptidases, regulatory and binding proteins. Smaller numbers of shared genes were associated with adherence^{21,23,28,32} ($n = 21$) and included transporters and membrane proteins; exosomes²⁹ ($n = 9$), including one core exosomal protein; and proteins of the secretome²⁷ ($n = 4$), and carbohydrate-active enzymes (CAZymes, $n = 1$) implicated as virulence factors³⁰.

A total of 138 of the 1201 genes with evidence of positive selection were found in *T. vaginalis*, and 69 of them are unique to the *T. vaginalis* lineage. While no GO terms were found to be enriched among them, ten genes (TVAGG3_0302500, TVAGG3_1001150, TVAGG3_1088290, TVAG_005750, TVAG_062520, TVAG_117090, TVAG_152520, TVAG_313880, TVAG_437950, TVAG_453350; Supplementary Data File 1) are specific to *T. vaginalis* and have experimentally verified functions associated with adherence^{21,22,24}, microvesicles²⁶, the secretome²⁷, phagocytosis²⁵, and CAZymes³⁰. *T. tenax* shows 45 genes with evidence of positive selection, 26 of which are unique to the lineage. We did not find GO enrichment among these 45 genes. However, six genes (TVAG_097660, TVAG_127300, TVAG_137880, TVAG_237760, TVAG_270770, TVAG_459530) under positive selection and shared between other trichomonad species have been associated with adherence²³, microvesicles²⁶, exosomes²⁹, and phagocytosis²⁵; all of these genes are shared with *T. vaginalis*.

Assuming that trichomonads have independently host-switched twice, from birds to humans to generate the *T. vaginalis* lineage, and from birds to mammals and humans to generate the *T. tenax* lineage⁹, and that selection will act on similar genes when different lineages independently adapt to similar environments, we applied the convergent evolution model RERconverge³³ to identify single-copy genes putatively involved in the transition to a mammalian/human host (Supplementary Data File 1). Of 6226 single-copy orthologs, 320 showed evidence of convergent purifying evolution in the human-



infecting branches *T. vaginalis* and *T. tenax*. Several of these genes are reported to be associated with phenotypes of phagocytosis²⁵ and adherence^{21,28}, as well as microvesicle²⁶ and exosome²⁹ structures, and CAZymes³⁰. A total of 93 single-copy orthologs showed evidence of convergent positive evolution in *T. vaginalis* and *T. tenax*; several of these have been reported to be involved in adherence²⁸, phagocytosis²⁵, and microvesicle-like structures²⁶.

Discussion

We present here a comparative analysis of chromosome-scale genomes of the human sexually transmitted parasite *T. vaginalis* with its sister species in birds, *T. stableri*. These are compared with genomes from five other species of human- and bird-infecting trichomonads. These comparisons illuminate differences in protein-coding gene and TE content, genomic architecture, and gene evolution across the

Fig. 4 | Analysis of orthologs across seven trichomonad species. **A** Graphs showing count of all single-copy orthologs (SCOs; left panel) and BUSCO genes (right panel) identified by RELAX as being under relaxed, neutral, or intensified selection in the species with expanded genomes (*T. vaginalis* and *T. tenax*) for a range of *P*-values. **B** Left panel: mean dN/dS values (plotted from 0.0 to 1.0) for SCOs under relaxed purifying selection for bird-infecting species ($n = 141$) and mammal-infecting species ($n = 31$), and right panel: dN/dS values (plotted from 1.0 to 100.0) for SCOs under relaxed positive selection for bird-infecting species

($n = 401$) and mammal-infecting species ($n = 104$). Boxplots represent the inter-quartile range (IQR) with the median as a horizontal line and whiskers extending to $1.5 \times$ IQR. For relaxed purifying selection, the mammal group had a Q1 of 0.38, median of 0.52, Q3 of 0.68, and whiskers from 0.09 to 0.98; the bird group had a Q1 of 0.38, median of 0.56, Q3 of 0.83, and whiskers from 0.08 to 1.00. For relaxed positive selection, the mammal group had a Q1 of 2.36, median of 5.79, Q3 of 33.92, and whiskers from 1.02 to 80.48; the bird group had a Q1 of 2.40, median of 7.32, Q3 of 31.15, and whiskers from 1.03 to 73.13.

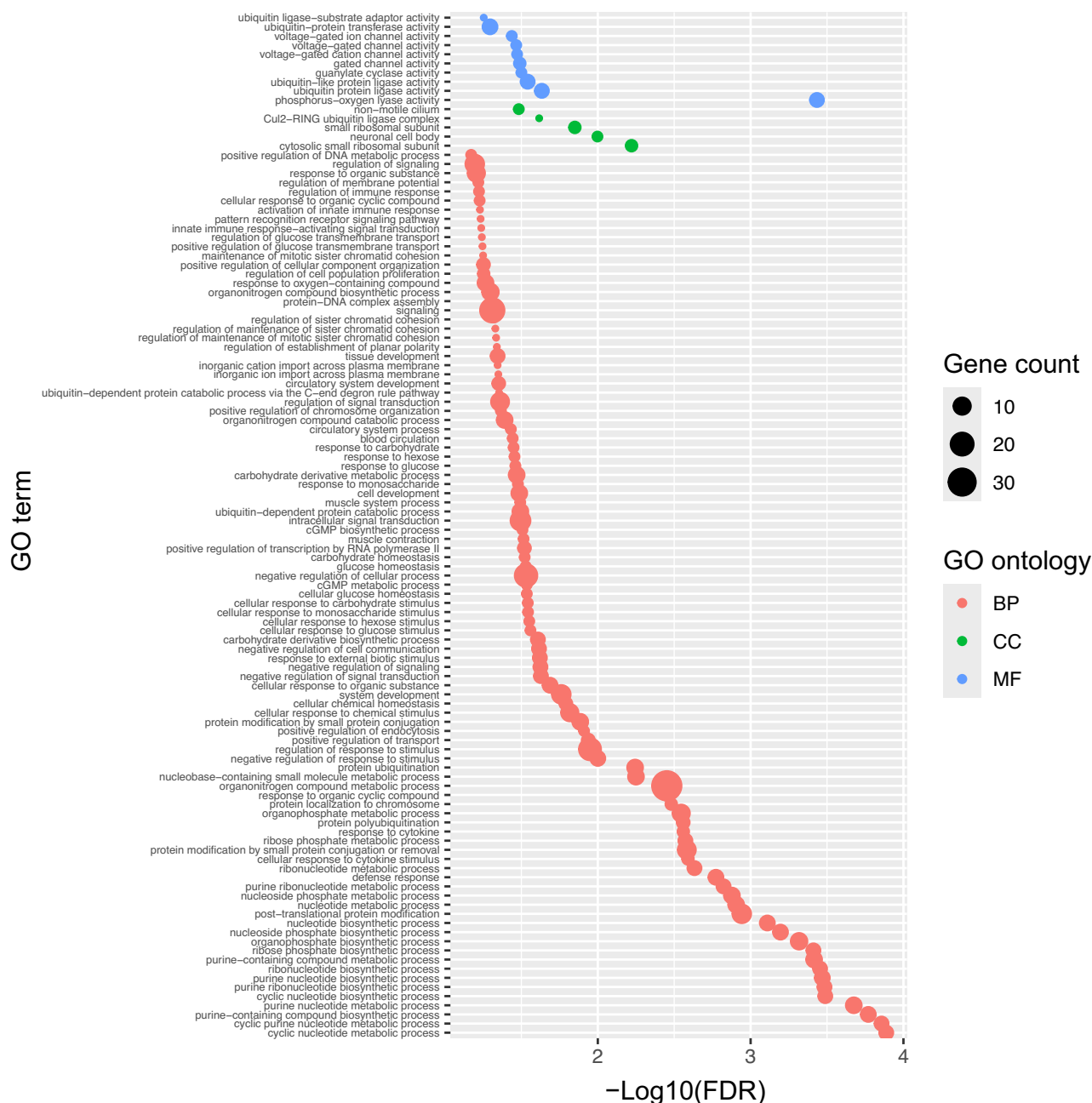


Fig. 5 | GO enrichment of 140 expanded gene families in *T. vaginalis*. Dot size represents the number of genes with a specific GO term. Biological process (BP), cellular component (CC), and molecular function (MF) are plotted. Only significant GO enrichments after FDR correction ($0.05 <$) are reported.

trichomonad phylogeny, and identify genes implicated in the inferred spillover event from avian to human host.

All of the trichomonads we sequenced have much larger genomes than other orders of single-celled parasites that cause important human diseases^{11,34}. The major contributor to increased genome size is

increased repeat content, in particular TE expansion, which has been proposed to be triggered by major environmental changes³⁵. TEs constitute the bulk of repetitive DNA in *T. vaginalis*, and likely the other genomes presented here as well. The presence of the same classes of TEs in all of the trichomonad genomes points to either

dosage balance, etc.) and assessing their functional roles in the parasite.

We previously hypothesized that the genome size expansion of *T. vaginalis* reflected a relaxation of selection when the parasite underwent a population size bottleneck during its transition from a GI environment to the urogenital tract¹⁰. In the present study, we found an overall trend of relaxed selection amongst human-infecting compared to bird-infecting trichomonad species, suggesting higher levels of genetic drift as a factor in their genome expansion. An intriguing question is whether host switch bottlenecks alone account for the relaxation of selection. Peters et al.⁹, estimated the co-divergence between columbid host and *Trichomonas* and observed relatively shallow branches in the parasite tree, indicating recent divergence in the parasites but not the hosts. Additionally, *T. gallinae*, and *T. sp. 2a* have been identified across bird orders, not just genera⁹. These observations suggest that recent host shifting, including across fairly large evolutionary distance, is a general phenomenon amongst columbid *Trichomonas*, and that we would therefore expect bottlenecks (and relaxed selection) in these species as well, if the hypothesis is true. But the relative lack of relaxed selection we observed in columbid *Trichomonas* overall (Fig. 4) suggests that factors other than bottlenecks contributed to the host-associated difference in selection strength. Mode of parasite reproduction is one such possible contributor. Asexual reproduction can lower the effective population size through decreased genetic variation and global reduction of variation due to background selection and genetic hitchhiking¹⁸. The last common ancestor to eukaryotes is thought to have reproduced sexually, and among extant eukaryotes sexual reproduction is generally the norm. We previously accumulated evidence that *T. vaginalis* may have undergone sexual recombination in its evolutionary past¹⁰; a putative hybridization event has also been described in *T. gallinae*⁴¹, raising the possibility that sex occurs in other *Trichomonas* species. Thus, it could be that a shift from sexual to asexual reproduction, in addition to a bottleneck, accompanied host switching, and facilitated relaxed selection, enabling large-scale structural changes to the genomes. Further investigation of reproduction in genus *Trichomonas* is needed to confirm this hypothesis.

Among the trichomonads in our study, we found the largest net gain in number of expanded multicopy gene families in *T. vaginalis*, and the highest number of gene family expansions shared with *T. vaginalis* in the *T. tenax*/*T. sp. 2a* clade, indicating that the latter similarity results from convergent evolution. The set of expanded families shared by *T. vaginalis* and human-infecting *T. tenax* is different from that shared by *T. vaginalis* and bird-infecting *T. sp. 2a*. Families that expanded in *T. vaginalis* and *T. tenax* feature more genes involved specifically in metabolism, cell adherence, microvesicles, and virulence, than those expanded/shared in *T. vaginalis* and *T. sp. 2a*, which could be evidence for human- (or at least mammal-) specific adaptations. Indeed, the diverse array of glycoside hydrolases, Carbohydrate Active enZymes (CAZymes), and carbohydrate-binding modules, identified through a recent comparative analysis of *T. vaginalis* and *T. tenax*³⁰ are likely shared virulence factors that potentially target host or bacterial glycans, and induce and/or amplify damaging inflammation and bacterial dysbiosis, known to exacerbate periodontitis and vaginitis. The functions associated with the shared *T. vaginalis*/*T. sp. 2a* families, on the other hand, could be those useful to parasitic trichomonads with bird-host ancestors. The recent reports of *T. tenax* in birds³ complicates this hypothesis. However, that report is based upon genotyping of the multicopy ITS1/5.8S/ITS2 rRNA small subunit gene, where discrimination between species can be based on as little as <=1% difference in sequence identity. Moreover, our *T. tenax* Hs-4:NIH genome sequence is of a strain isolated from a human subject and presumably adapted to that host. *T. tenax* has also been isolated

from a range of birds and mammals such as cats, dogs, and horses³, raising the possibility that the ancestor of *T. tenax* was transmitted from birds to mammals before jumping to humans. The recently identified *Trichomonas bixi*⁴² appears to have undergone a similar bird-to-mammal transmission event, an interesting parallel. More sequence data of *T. tenax* isolates from humans, other mammals, and birds are needed to clarify this. The columbid upper GI tract and the oral and vaginal cavities of humans are lined with stratified, non-cornified epithelia^{43,44}, a histological similarity that conceivably enabled the ancestral colonization of a human tissue by a bird trichomonad. At the same time, convergent changes in the human-infective species suggest there was enough microscale difference in the host environments to drive adaptation. Convergently evolving multicopy gene families in *T. vaginalis* and *T. tenax* included some associated with cell adherence, suggesting specifically that differences in surface membrane proteins in bird versus human mucosal epithelium could foster selection for differential adherence to host tissues.

Multicopy genes are challenging to use in some evolutionary analyses because it is difficult to identify orthologues between them. But evidence from analysis of single-copy gene evolution can illuminate phenomena such as host-switching or spillover. For this analysis we looked at single-copy orthologues two ways: (1) specifically for positive selection, and (2) more generally for rates of evolution, since convergent evolutionary rate shifts can indicate whether changes in selection in a gene cohort are due to purifying selection versus relaxed or positive selection compared to the average rate across the phylogeny. Most of the single-copy genes we found with evidence for positive selection were species-specific, suggesting fine-tuning of the parasite to particular environments. However, the single-copy orthologues in *T. vaginalis* and *T. tenax* we identified as displaying convergent purifying or positive evolution were often related to the endo- and cell membrane systems, and also to adherence, phagocytosis, and mitosis. The endomembrane system generates extracellular vesicles, e.g., exosomes and microvesicles, which have recently been identified in *T. vaginalis* and shown to prime host cells for adherence, modulate the host's immune response, facilitate cell-to-cell communication, and promote host cell colonization^{22,24,26,29}. Convergent selection for endomembrane system genes could reflect adaptation of the parasite to new host cell surface membranes and immune system; vesicles can carry cargo that affect host gene expression, and the removal of these vesicles from the extracellular milieu reduces the adherence of the parasite to host cells²². Parasite adherence to host mucosal cells is essential in establishing an infection, and parasite phagocytosis is involved in nutrient acquisition⁴⁵ and immune cell evasion⁴⁶. Autophagy is associated with the pathogenicity of several protozoan parasites and has been demonstrated to increase the survivability of *T. vaginalis* under nutrient starvation⁴⁷ as well as participate in proteolysis⁴⁸. Both phagocytosis and autophagy also involve the endomembrane system. Peculiarly among eukaryotes, *T. vaginalis* mitosis can occur during phagocytosis, which has been hypothesized to be advantageous for a parasite in a hostile environment with scarce nutrients⁴⁹. In conclusion, our results implicate several genes and gene families involved in parasite adherence, phagocytosis, and microvesicle-like structures in the spillover of parasites from the upper GI tract of columbids into the human reproductive tract. This analysis provides candidates for further investigation into trichomonad evolution and adaptation to human hosts.

Methods

Generation of a *T. vaginalis* chromosome-scale assembly and annotation

DNA was extracted from *T. vaginalis* strain G3 parasites cultured in modified Diamond's media and sequenced using Pacific Biosciences

Inc. sequencing chemistry on 56 SMRT cells on a PacBio RSII instrument, generating 2,043,705,869 reads that were initially assembled using FALCON⁵⁰. The initial assembly had a total span of 173 Mb across 1194 contigs with a contig N50 size of 321 Kb. Hi-C library preparation and sequencing were performed as described⁵¹, and PBjelly⁵² run to close any scaffold gaps. In total, this yielded six chromosome-scale scaffolds containing 97.4% of the original assembly with a scaffold N50 size of 27.3 Mb, scaffold N90 size of 20.0 Mb, and improved the contig N50 size to 444 Kb. Pilon⁵³ was used for assembly polishing two times using published G3 Illumina reads (SRA# SRR4734558), Sanger reads¹⁰, and RNA-seq reads³⁷ mapped to the assembly using BWA⁵⁴.

Structural annotation used BRAKER2⁵⁵, STAR⁵⁶-mapped RNA-seq reads, and a training set of 539 high-confidence *T. vaginalis* protein sequences. De novo structural annotation was augmented by gene model transfer from the 2007 *T. vaginalis* assembly (TrichDB release 52), using LiftOff⁵⁷ with parameters *-s 0.9* and *-a 0.9*. Functional annotation used one of six criteria: (1) identity to proteins with previously experimentally characterized function; (2) identity to proteins previously inferred as horizontally transferred from firmicute bacterium *Peptoniphilus harei*⁴⁵; (3) strong similarity (90% identity over 90% length) to UniProtKB/Swissprot entries; (4) orthology group membership and function using eggNOG-mapper⁵⁸ and the eggNOG database of orthology groups⁵⁹; (5) protein domains returned by Interproscan (v 5.52.86)⁶⁰; (6) DeepFRI function prediction from predicted protein structure⁶¹; and for the remainder (6) DeepGOPlus⁶² version 1.0.20 function prediction. Proteins that could not be assigned a function by these means were called ‘conserved hypothetical’. GO enrichment analysis was undertaken using the hypergeometric distribution incorporated into an inhouse Python script.

Maverick TEs were identified by BLAST using ORFs from 11 ‘canonical’ Mavericks identified previously¹⁶. Ordered blocks of Maverick ORFs were marked in the polished assembly. Canonical and novel TIRs flanking the blocs were identified with BLAST and Inverted Repeats Finder⁶³. Other TE families were identified through BLASTn queries using consensus TE sequences from Repbase⁶⁴, GyDB⁶⁵, and a custom database of previously identified TEs (Supplementary Data File 2); RepeatModeler2⁶⁶ was used to identify novel potential TEs. We used phylogenetic analysis, motif identification, and Interproscan to validate the classification of RepeatModeler TE consensus, and everted (EMBOSS⁶⁷) and GenericRepeatFinder⁶⁸ to annotate TIRs and target site duplications followed by manual inspection of a multiple sequence alignment of the TE family.

Sequencing, assembly, and annotation of six additional trichomonad species

T. gallinae strain TGAL (see Supplementary Methods), *Trichomonas* species genotype 1c, *Trichomonas* species genotype 2a, *T. tenax* strain Hs-4:NIH (ATCC 30207), *P. hominis* strain Hs-3:NIH (ATCC 30000), *T. stableri* strains CA015840 (ATCC PRA-430) and BTPI-3 (ATCC PRA-412), and two strains of *T. vaginalis* CDC 085 (ATCC 50143) and NYH 286 (ATCC 50148) were grown axenically in vitro under standard conditions, DNA extracted, libraries generated, and sequenced on an Illumina HiSeq platform. Barcode sequences were trimmed using the fastx toolkit (https://github.com/agordon/fastx_toolkit), sequencing errors were corrected using Quake⁶⁹ and then assembled using SOAPdenovo2⁷⁰, yielding contig N50 sizes of 10 Kb to 25 Kb (Table 1). Genome sizes were estimated from Illumina reads using GenomeScope⁷¹. *T. stableri* strains BTPI-3 and CA015840 were sequenced using Pacific Biosciences Sequel II SMRT technology, assembled using hierarchical genome-assembly HGAP (Pacific Biosciences, SMRT Link V11.1) and Canu⁷², and the resulting assemblies scaffolded using Hi-C data⁵¹. RNA-seq data were generated in triplicate for *T. stableri* strains BTPI-3 and CA015840, using total RNA extracted from three biological replicate cultures for each strain, stranded mRNA preparation, and the resulting libraries run in HighOutput mode on a

NextSeq 500 sequencer to produce 2 × 75 bp paired-end reads. TE expression was estimated in *T. stableri* as for *T. vaginalis* G3 above.

De novo gene finding and annotation of the remaining five assemblies was performed using AUGUSTUS⁷³ with ab initio training using the standard translation code. RNA-seq data were used for transcript assembly and annotation, where available for each species, and annotation was manually curated when possible. For annotation of TEs, we used BLASTn⁷⁴ with conserved sequence motifs of all TE consensus sequences identified in *T. stableri* and *T. vaginalis* as queries. For the other species, their lower assembly quality precluded annotation of TE sequences. To quantify them, TE queries based on *T. vaginalis*/*T. stableri* consensus sequences were used in BLASTn to find matches in each species, which were used to generate per-species consensus sequences. Raw reads were mapped to these consensus sequences using deviateTE⁷⁵, to estimate the true insertion frequency of each TE family except Mavericks, where raw reads mapping to the integrase ORF were used to estimate TE frequency.

Comparative genomics

DNA sequence similarity across the seven *Trichomonas* species at the whole genome level was calculated using MUMmer v.3.23 dnadiff algorithm⁷⁶ using default parameters, and Bray-Curtis dissimilarity statistics. Synteny analysis was determined using MScanX⁷⁷ using default parameters (Maximum Evalue: 1e-10, Num. of BlastHits: 5 [minimum collinearity length]), which identified collinear blocks consists of ≥ five genes conserved between the two species. OrthoFinder⁷⁸ was used to identify 6,226 single-copy orthologs (SCOs) across the seven trichomonad species, and GO terms assigned to them using embedding similarity⁷⁹. Other analyses used custom in-house Python Scripts and packages in R, such as UpSetR in version 1.3.3; 2017.

Phylogenetic and evolutionary analyses

A species tree of the seven trichomonad species was generated from 6226 genes present in one copy in each genome (‘single-copy orthologues’). Orthologues were aligned using PRANK⁸⁰ with default parameters and concatenated to generate a supergene matrix for phylogenetic inference with Phangorn⁸¹, estimating the best evolution model as GTR + G + I using AICc and executing 1000 bootstraps for analysis. To test if expanded genomes experienced genome-wide relaxed selection, we used RELAX¹⁷ on the 6226 single-copy orthologs. We tested human-infecting *Trichomonas* species (*T. vaginalis* and *T. tenax*) with the four avian-infecting species set as background, and the outgroup *P. hominis* excluded. We tested the avian sister species (*T. stableri* and *T. sp.* genotype 2a) of *T. vaginalis* and *T. tenax* against all *Trichomonas* species (i.e., excluding *P. hominis*). BUSCO¹⁹ was used to identify single-copy orthologs that are near-universal across eukaryotes. Significant genes in RELAX results were searched against a curated database of published papers associated with specific phenotypes such as virulence (Supplementary Data File 3). CAFES²⁰ was used to implement a birth-death model for evolutionary inferences about gene family evolution. A total of 12,345 of 26,244 orthogroups were tested that met the CAFE requirement that each orthogroup include the outgroup species *P. hominis*. The R package RERConverge³³ was used to test for association between relative evolutionary rates of genes and the evolution of traits across the phylogeny. We performed the association by designating human-infecting *Trichomonas* species (excluding *P. hominis*) as the foreground against all bird-infecting species for all 6226 single-copy genes. We assessed significance using permutations, phylogenetic simulations and trait permutation, with RERconverge. This enabled the generation of a list of candidate genes associated with host type. aBRASEL³¹ was used to test for positive selection in all 6226 single-copy genes across all *Trichomonas* species using default parameters without a priori selection of foreground branches.

Reporting summary

Further information on research design is available in the Nature Portfolio Reporting Summary linked to this article.

Data availability

Data supporting the findings of this work are available within the paper and its Supplementary Information files. The raw sequence data have been deposited in GenBank under the following accession numbers: *T. vaginalis* strain G3: Bio-Project PRJNA885811, Genome Accession SAMN31107788, RNA-Seq SUB12510628; *T. vaginalis* strain CDC 085: SRA SRX1017343, SRX1017342; *T. vaginalis* strain NYH 286: SRA SRX1017345, SRX1017344; *T. stableri* strain BTPI-3: Bio-Project PRJNA816543, Genome SUB11194301, RNA-seq SUB12511058; *T. stableri* strain CA015840: Bio-Project PRJNA828130, Genome SUB11350628, RNA-seq SUB12511233, Illumina DNA-seq reads SRA SRR30350957; *T. gallinae* strain TGAL: Bio-Project PRJNA885811, Genome SUB14002162; *Trichomonas* species genotype 1c: Bio-Project PRJNA885811, Genome: SUB14002711; *Trichomonas* species genotype 2a: Bio-Project PRJNA885811, Genome SUB14002751; *T. tenax* strain Hs-4:NIH: Bio-Project PRJNA885811, Genome: SUB14002737; *P. hominis* strain Hs-3:NIH: Bio-Project PRJNA885811, Genome SUB14002786. The source data underlying the figures and tables are provided as a Source Data File. Icons used in figures and tables were from Adobe Stock and Microsoft Stock which are copyright-free. Source data are provided with this paper.

Code availability

Code for *T. vaginalis* GO enrichment is available at <https://github.com/biofallejas/TriGO> and is permanently referenced with the link <https://doi.org/10.5281/zenodo.15002692>.

References

1. Van Gerwen, O. T. & Muzny, C. A. Recent advances in the epidemiology, diagnosis, and management of *Trichomonas vaginalis* infection. *F1000Res*. **8**, F1000 (2019).
2. Van Gerwen, O. T., Muzny, C. A. & Marrazzo, J. M. Sexually transmitted infections and female reproductive health. *Nat. Microbiol.* **7**, 1116–1126 (2022).
3. Matthew, M. A., Yang, N., Ketzis, J., Mukaratirwa, S. & Yao, C. *Trichomonas tenax*: a neglected protozoan infection in the oral cavities of humans and dogs—A scoping review. *Trop. Med. Infect. Dis.* **8**, 60 (2023).
4. Zhang, N. et al. High prevalence of *Pentatrichomonas hominis* infection in gastrointestinal cancer patients. *Parasit. Vectors* **12**, 423 (2019).
5. Stabler, R. M. *Trichomonas gallinae*: a review. *Exp. Parasitol.* **3**, 368–402 (1954).
6. Lawson, B. et al. A clonal strain of *Trichomonas gallinae* is the aetiological agent of an emerging avian epidemic disease. *Infect. Genet. Evol.* **11**, 1638–1645 (2011).
7. Gerhold, R. W. et al. Molecular characterization of the *Trichomonas gallinae* morphological complex in the United States. *J. Parasitol.* **94**, 1335–1341 (2008).
8. Girard, Y. A. et al. *Trichomonas stableri* n. sp., an agent of trichomonosis in Pacific Coast band-tailed pigeons (*Patagioenas fasciata monilis*). *Int. J. Parasitol. Parasites Wildl.* **3**, 32–40 (2014).
9. Peters, A., Das, S. & Raidal, S. R. Diverse *Trichomonas* lineages in Australasian pigeons and doves support a columbid origin for the genus *Trichomonas*. *Mol. Phylogenet. Evol.* **143**, 106674 (2020).
10. Carlton, J. M. et al. Draft genome sequence of the sexually transmitted pathogen *Trichomonas vaginalis*. *Science* **315**, 207–212 (2007).
11. Barratt, J., Gough, R., Stark, D. & Ellis, J. Bulky trichomonad genomes: encoding a swiss army knife. *Trends Parasitol.* **32**, 783–797 (2016).
12. Malik, S. B. et al. Phylogeny of parasitic parabasalia and free-living relatives inferred from conventional markers vs. Rpb1, a single-copy gene. *PLoS ONE* **6**, e20774 (2011).
13. Yuh, Y. S., Liu, J. Y. & Shao, M. F. Chromosome number of *Trichomonas vaginalis*. *J. Parasitol.* **83**, 551–553 (1997).
14. Conrad, M. et al. Microsatellite polymorphism in the sexually transmitted human pathogen *Trichomonas vaginalis* indicates a genetically diverse parasite. *Mol. Biochem. Parasitol.* **175**, 30–38 (2011).
15. Strese, A., Backlund, A. & Alsmark, C. A recently transferred cluster of bacterial genes in *Trichomonas vaginalis*—lateral gene transfer and the fate of acquired genes. *BMC Evol. Biol.* **14**, 119 (2014).
16. Pritham, E. J., Putliwala, T. & Feschotte, C. Mavericks, a novel class of giant transposable elements widespread in eukaryotes and related to DNA viruses. *Gene* **390**, 3–17 (2007).
17. Wertheim, J. O., Murrell, B., Smith, M. D., Kosakovsky Pond, S. L. & Scheffler, K. RELAX: detecting relaxed selection in a phylogenetic framework. *Mol. Biol. Evol.* **32**, 820–832 (2015).
18. Glemin, S., Francois, C. M. & Galtier, N. Genome evolution in outcrossing vs. selfing vs. asexual species. *Methods Mol. Biol.* **1910**, 331–369 (2019).
19. Manni, M., Berkeley, M. R., Seppey, M., Simao, F. A. & Zdobnov, E. M. BUSCO update: novel and streamlined workflows along with broader and deeper phylogenetic coverage for scoring of eukaryotic, prokaryotic, and viral genomes. *Mol. Biol. Evol.* **38**, 4647–4654 (2021).
20. Mendes, F. K., Vanderpool, D., Fulton, B. & Hahn, M. W. CAFE 5 models variation in evolutionary rates among gene families. *Bioinformatics* **36**, 5516–5518 (2021).
21. de Miguel, N. et al. Proteome analysis of the surface of *Trichomonas vaginalis* reveals novel proteins and strain-dependent differential expression. *Mol. Cell Proteom.* **9**, 1554–1566 (2010).
22. Kochanowsky, J. A. et al. *Trichomonas vaginalis* extracellular vesicles up-regulate and directly transfer adherence factors promoting host cell colonization. *Proc. Natl. Acad. Sci. USA* **121**, e2401159121 (2024).
23. Molgora, B. M. et al. A novel *trichomonas vaginalis* surface protein modulates parasite attachment via protein: host cell proteoglycan interaction. *mBio* **12**, e03374–20 (2021).
24. Nieves, Y. R. et al. Extracellular vesicles released by anaerobic protozoan parasites: current situation. *Cell Microbiol.* **22**, e13257 (2020).
25. Zimmann, N. et al. Proteomic analysis of *Trichomonas vaginalis* phagolysosome, lysosomal targeting, and unconventional secretion of cysteine peptidases. *Mol. Cell Proteom.* **21**, 100174 (2022).
26. Nieves, Y. R. et al. Membrane-shed vesicles from the parasite *Trichomonas vaginalis*: characterization and their association with cell interaction. *Cell Mol. Life Sci.* **75**, 2211–2226 (2018).
27. Stafkova, J. et al. Dynamic secretome of *Trichomonas vaginalis*: case study of beta-amylases. *Mol. Cell Proteom.* **17**, 304–320 (2018).
28. Nieves, Y. R. et al. Protein palmitoylation plays an important role in *Trichomonas vaginalis* adherence. *Mol. Cell Proteom.* **17**, 2229–2241 (2018).
29. Twu, O. et al. *Trichomonas vaginalis* exosomes deliver cargo to host cells and mediate hostratioparasite interactions. *PLoS Pathog.* **9**, e1003482 (2013).
30. Mpeyako, L. A. et al. Comparative genomics between *Trichomonas tenax* and *Trichomonas vaginalis*: CAZymes and candidate virulence factors. *Front. Microbiol.* **15**, 1437572 (2024).
31. Smith, M. D. et al. Less is more: an adaptive branch-site random effects model for efficient detection of episodic diversifying selection. *Mol. Biol. Evol.* **32**, 1342–1353 (2015).
32. Coceres, V. M. et al. The C-terminal tail of tetraspanin proteins regulates their intracellular distribution in the parasite *Trichomonas vaginalis*. *Cell Microbiol.* **17**, 1217–1229 (2015).

33. Kowalczyk, A. et al. RERconverge: an R package for associating evolutionary rates with convergent traits. *Bioinformatics* **35**, 4815–4817 (2019).
34. Zubacova, Z., Cimburek, Z. & Tachezy, J. Comparative analysis of trichomonad genome sizes and karyotypes. *Mol. Biochem. Parasitol.* **161**, 49–54 (2008).
35. Piacentini, L. et al. Transposons, environmental changes, and heritable induced phenotypic variability. *Chromosoma* **123**, 345–354 (2014).
36. Bradic, M., Warring, S. D., Low, V. & Carlton, J. M. The Tc1/mariner transposable element family shapes genetic variation and gene expression in the protist *Trichomonas vaginalis*. *Mob. DNA* **5**, 12 (2014).
37. Warring, S. D. et al. Small RNAs are implicated in regulation of gene and transposable element expression in the protist *Trichomonas vaginalis*. *mSphere* **6**, e01061–20 (2021).
38. Birchler, J. A. & Yang, H. The multiple fates of gene duplications: deletion, hypofunctionalization, subfunctionalization, neofunctionalization, dosage balance constraints, and neutral variation. *Plant Cell* **34**, 2466–2474 (2022).
39. Lynch, M. *The Origins of Genome Architecture* (Sunderland, Sinauer Associates, Inc., 2007).
40. Bradic, M. & Carlton, J. M. Does the common sexually transmitted parasite *Trichomonas vaginalis* have sex?. *PLoS Pathog.* **14**, e1006831 (2018).
41. Alrefaei, A. F. et al. Multilocus analysis resolves the European finch epidemic strain of *Trichomonas gallinae* and suggests introgression from divergent trichomonads. *Genome Biol. Evol.* **11**, 2391–2402 (2019).
42. Kellerova, P. & Tachezy, J. Zoonotic *Trichomonas tenax* and a new trichomonad species, *Trichomonas brixi* n. sp., from the oral cavities of dogs and cats. *Int. J. Parasitol.* **47**, 247–255 (2017).
43. Bragulla, H. H. & Homberger, D. G. Structure and functions of keratin proteins in simple, stratified, keratinized and cornified epithelia. *J. Anat.* **214**, 516–559 (2009).
44. Mahdy, M. A. A. & Mohammed, E. S. I. Anatomical, histological, and scanning electron microscopic features of the esophagus and crop in young and adult domestic pigeons (*Columba livia Domestica*). *BMC Vet. Res.* **20**, 428 (2024).
45. Midleij, V. & Benchimol, M. *Trichomonas vaginalis* kills and eats—evidence for phagocytic activity as a cytopathic effect. *Parasitology* **137**, 65–76 (2010).
46. Mercer, F. et al. Leukocyte lysis and cytokine induction by the human sexually transmitted parasite *Trichomonas vaginalis*. *PLoS Negl. Trop. Dis.* **10**, e0004913 (2016).
47. Huang, K. Y. et al. Adaptive responses to glucose restriction enhance cell survival, antioxidant capability, and autophagy of the protozoan parasite *Trichomonas vaginalis*. *Biochim. Biophys. Acta* **1840**, 53–64 (2014).
48. Huang, K. Y. et al. Potential role of autophagy in proteolysis in *Trichomonas vaginalis*. *J. Microbiol. Immunol. Infect.* **52**, 336–344 (2019).
49. Pereira-Neves, A. & Benchimol, M. Phagocytosis by *Trichomonas vaginalis*: new insights. *Biol. Cell* **99**, 87–101 (2007).
50. Chin, C. S. et al. Phased diploid genome assembly with single-molecule real-time sequencing. *Nat. Methods* **13**, 1050–1054 (2016).
51. Burton, J. N. et al. Chromosome-scale scaffolding of de novo genome assemblies based on chromatin interactions. *Nat. Biotechnol.* **31**, 1119–1125 (2013).
52. English, A. C. et al. Mind the gap: upgrading genomes with Pacific Biosciences RS long-read sequencing technology. *PLoS ONE* **7**, e47768 (2012).
53. Walker, B. J. et al. Pilon: an integrated tool for comprehensive microbial variant detection and genome assembly improvement. *PLoS ONE* **9**, e112963 (2014).
54. Li, H. & Durbin, R. Fast and accurate short read alignment with Burrows-Wheeler transform. *Bioinformatics* **25**, 1754–1760 (2009).
55. Bruna, T., Hoff, K. J., Lomsadze, A., Stanke, M. & Borodovsky, M. BRAKER2: automatic eukaryotic genome annotation with GeneMark-EP+ and AUGUSTUS supported by a protein database. *NAR Genom. Bioinform.* **3**, lqaa108 (2021).
56. Dobin, A. et al. STAR: ultrafast universal RNA-seq aligner. *Bioinformatics* **29**, 15–21 (2013).
57. Shumate, A. & Salzberg, S. L. Liftoff: accurate mapping of gene annotations. *Bioinformatics* **37**, 1639–1643 (2021).
58. Huerta-Cepas, J. et al. Fast genome-wide functional annotation through orthology assignment by eggNOG-mapper. *Mol. Biol. Evol.* **34**, 2115–2122 (2017).
59. Huerta-Cepas, J. et al. eggNOG 5.0: a hierarchical, functionally and phylogenetically annotated orthology resource based on 5090 organisms and 2502 viruses. *Nucleic Acids Res.* **47**, D309–D314 (2019).
60. Paysan-Lafosse, T. et al. InterPro in 2022. *Nucleic Acids Res.* **51**, D418–D427 (2023).
61. Gligorijevic, V. et al. Structure-based protein function prediction using graph convolutional networks. *Nat. Commun.* **12**, 3168 (2021).
62. Kulmanov, M., Zhapa-Camacho, F. & Hoehndorf, R. DeepGOWeb: fast and accurate protein function prediction on the (Semantic) Web. *Nucleic Acids Res.* **49**, W140–W146 (2021).
63. Warburton, P. E., Giordano, J., Cheung, F., Gelfand, Y. & Benson, G. Inverted repeat structure of the human genome: the X-chromosome contains a preponderance of large, highly homologous inverted repeats that contain testes genes. *Genome Res.* **14**, 1861–1869 (2004).
64. Bao, W., Kojima, K. K. & Kohany, O. Repbase update, a database of repetitive elements in eukaryotic genomes. *Mob. DNA* **6**, 11 (2015).
65. Hafez, A. I. et al. Client applications and server-side Docker for management of RNASeq and/or VariantSeq workflows and pipelines of the GPRO suite. *Genes (Basel)* **14**, 267 (2023).
66. Flynn, J. M. et al. RepeatModeler2 for automated genomic discovery of transposable element families. *Proc. Natl. Acad. Sci. USA* **117**, 9451–9457 (2020).
67. Rice, P., Longden, I. & Bleasby, A. EMBOSS: the European molecular biology open software suite. *Trends Genet.* **16**, 276–277 (2000).
68. Shi, J. & Liang, C. Generic repeat finder: a high-sensitivity tool for genome-wide de novo repeat detection. *Plant Physiol.* **180**, 1803–1815 (2019).
69. Kelley, D. R., Schatz, M. C. & Salzberg, S. L. Quake: quality-aware detection and correction of sequencing errors. *Genome Biol.* **11**, R116 (2010).
70. Luo, R. et al. SOAPdenovo2: an empirically improved memory-efficient short-read de novo assembler. *Gigascience* **1**, 18 (2012).
71. Ranallo-Benavidez, T. R., Jaron, K. S. & Schatz, M. C. GenomeScope 2.0 and Smudgeplot for reference-free profiling of polyploid genomes. *Nat. Commun.* **11**, 1432 (2020).
72. Koren, S. et al. Canu: scalable and accurate long-read assembly via adaptive k-mer weighting and repeat separation. *Genome Res.* **27**, 722–736 (2017).
73. Stanke, M. & Waack, S. Gene prediction with a hidden Markov model and a new intron submodel. *Bioinformatics* **19**, ii215–ii225 (2003).
74. Altschul, S. F., Gish, W., Miller, W., Myers, E. W. & Lipman, D. J. Basic local alignment search tool. *J. Mol. Biol.* **215**, 403–410 (1990).
75. Weigluny, L. & Kofler, R. DeviaTE: assembly-free analysis and visualization of mobile genetic element composition. *Mol. Ecol. Resour.* **19**, 1346–1354 (2019).
76. Kurtz, S. et al. Versatile and open software for comparing large genomes. *Genome Biol.* **5**, R12 (2004).
77. Wang, Y. et al. MCScanX: a toolkit for detection and evolutionary analysis of gene synteny and collinearity. *Nucleic Acids Res.* **40**, e49 (2012).

78. Emms, D. M. & Kelly, S. OrthoFinder: phylogenetic orthology inference for comparative genomics. *Genome Biol.* **20**, 238 (2019).
79. Littmann, M., Heininger, M., Dallago, C., Olenyi, T. & Rost, B. Embeddings from deep learning transfer GO annotations beyond homology. *Sci. Rep.* **11**, 1160 (2021).
80. Loytynoja, A. Phylogeny-aware alignment with PRANK. *Methods Mol. Biol.* **1079**, 155–170 (2014).
81. Schliep, K. P. phangorn: phylogenetic analysis in R. *Bioinformatics* **27**, 592–593 (2011).

Acknowledgements

We thank Mari Shiratori, Sally D. Warring, Martina Bradic, Akash Sookdeo, Charlotte Darby, and Srividya Ramakrishnan for initial wet lab and genome analyses. We thank Ellen Pritham for supplying canonical Maverick sequences. Research reported in this publication was partially supported by: the NYU IT High Performance Computing resources, services, and staff expertise; CMRPD1M0571-2 from Chang Gung Memorial Hospital and NSTC-110-2320B-182-016-MY3 from National Science and Technology Council, Taiwan; Australian Government Wildlife Exotic Disease Preparedness Program; and the National Institute Of Allergy And Infectious Diseases of the National Institutes of Health under Award Number R21AI149449 and U24AI183870. The content is solely the responsibility of the authors and does not necessarily represent the official views of the National Institutes of Health.

Author contributions

J.M.C. and M.C.S. designed the study, provided the funding for resequencing *T. vaginalis*, supervised the work, and interpreted the analyses. Y.A.G., C.K.J., K.H.R. and R.G. provided *Trichomonas* isolates. P.-J.H., Y.-M.Y., C.-C.L., H.L., T.-W.C., P.T. and C.-H.C. provided the *T. tenax*, *P. hominis*, *T. stableri* CA015840, *T. vaginalis* strain CDC O85, and *T. vaginalis* strain NYH 286 Illumina whole genome sequence data, and A.P. and S.R.R. provided the *T. gallinae* TGAL, *T. sp.* genotype 1c, and *T. sp.* genotype 2a Illumina whole genome sequence data. S.A.S., J.C.O., F.C.-H., F.B., T.R.R.-B. and H.L. undertook genome annotation and analysis, and additionally F.B. and F.C.-H. generated the *T. stableri* BTPI-3 genome sequence and undertook wet lab work. H.M. and I.L. undertook Hi.-C. H.S., C.C., D.B., V.G. and R.A.B. helped with *T. vaginalis* functional annotation. All authors contributed to the writing of the manuscript and approved the final version before submission.

Competing interests

I.L. and H.M. are employees of Phase Genomics, a company that provides Hi-C services and products. The following author wishes to disclose his industry relations although there are no competing interests to the work published here: R.A.B. is an employee of Genentech/Roche. The remaining authors declare no competing interests.

Additional information

Supplementary information The online version contains supplementary material available at <https://doi.org/10.1038/s41467-025-61483-w>.

Correspondence and requests for materials should be addressed to Jane M. Carlton.

Peer review information *Nature Communications* thanks Neil Young and the other, anonymous, reviewer(s) for their contribution to the peer review of this work. A peer review file is available.

Reprints and permissions information is available at <http://www.nature.com/reprints>

Publisher's note Springer Nature remains neutral with regard to jurisdictional claims in published maps and institutional affiliations.

Open Access This article is licensed under a Creative Commons Attribution-NonCommercial-NoDerivatives 4.0 International License, which permits any non-commercial use, sharing, distribution and reproduction in any medium or format, as long as you give appropriate credit to the original author(s) and the source, provide a link to the Creative Commons licence, and indicate if you modified the licensed material. You do not have permission under this licence to share adapted material derived from this article or parts of it. The images or other third party material in this article are included in the article's Creative Commons licence, unless indicated otherwise in a credit line to the material. If material is not included in the article's Creative Commons licence and your intended use is not permitted by statutory regulation or exceeds the permitted use, you will need to obtain permission directly from the copyright holder. To view a copy of this licence, visit <http://creativecommons.org/licenses/by-nc-nd/4.0/>.

© The Author(s) 2025

¹Center for Genomics and Systems Biology, Department of Biology, New York University, New York, NY, USA. ²Department of Molecular Microbiology and Immunology, Bloomberg School of Public Health, Johns Hopkins University, Baltimore, MD, USA. ³Simons Center for Quantitative Biology, Cold Spring Harbor Laboratory, Cold Spring Harbor, NY, USA. ⁴Department of Computer Science, Whiting School of Engineering, Johns Hopkins University, Baltimore, MD, USA. ⁵School of Agricultural, Environmental and Veterinary Sciences, Charles Sturt University, Wagga Wagga, NSW, Australia. ⁶Melbourne Veterinary School, The University of Melbourne, Melbourne, VIC, Australia. ⁷One Health Institute, School of Veterinary Medicine, University of California, Davis, Davis, CA, USA. ⁸Wildlife Health Laboratory, California Department of Fish & Wildlife, Sacramento, CA, USA. ⁹Department of Biomedical and Diagnostic Sciences, College of Veterinary Medicine, University of Tennessee, Knoxville, TN, USA. ¹⁰Phase Genomics, Seattle, WA, USA. ¹¹Courant Institute, Department of Computer Science, New York University, New York, NY, USA. ¹²Molecular Medicine Research Center, Chang Gung University, Taoyuan, Taiwan. ¹³Molecular Infectious Disease Research Center, Chang Gung Memorial Hospital, Linkou, Taoyuan, Taiwan. ¹⁴Department of Biomedical Engineering, Johns Hopkins University, Baltimore, MD, USA. ¹⁵Present address: School of Infection and Immunity, College of Medical, Veterinary and Life Sciences, University of Glasgow, Glasgow, UK. ¹⁶Present address: Cancer Epigenetics Institute, Fox Chase Cancer Center, Philadelphia, PA, USA. ¹⁷Present address: Translational Genomics Research Institute, Phoenix, AZ, USA. ¹⁸Present address: MRIGlobal, Kansas City, MO, USA. ¹⁹Present address: Genentech/Roche, South San Francisco, CA, USA. ²⁰Present address: Genomic Medicine Core Laboratory, Chang Gung Memorial Hospital, Linkou, Taoyuan, Taiwan. ²¹Present address: Department of Biological Science and Technology, National Yang Ming Chiao Tung University, Hsinchu, Taiwan. ²²These authors contributed equally: Steven A. Sullivan, Jordan C. Orocco. ✉ e-mail: JaneCarlton@jhu.edu